Phase Separation Behavior in Tough and Self-Healing Polyampholyte Hydrogels

Kunpeng Cui[1], Ya Nan Ye[2], Tao Lin Sun[2,3,4], Chengtao Yu[5], Xueyu Li[2], Takayuki Kurokawa[2,3], Jian Ping Gong[1,2,3*]

[1]*Institute for Chemical Reaction Design and Discovery (WPI-ICReDD), Hokkaido University, Sapporo 001-0021, Japan*

[2]*Soft Matter GI-CoRE, Hokkaido University, Sapporo 001-0021, Japan*

[3]*Faculty of Advanced Life Science, Hokkaido University, Sapporo 060-0810, Japan*

[4]*South China Advanced Institute for Soft Matter Science and Technology, South China University of Technology, Guangzhou 510640, China*

[5]*Graduate School of Life Science, Hokkaido University, Sapporo 060-0810, Japan*

*Corresponding author: gong@sci.hokudai.ac.jp

ABSTRACT

Polyampholyte hydrogels (PA gels) are drawing great attention for their excellent mechanical properties including self-healing, high toughness and fatigue resistance. These mechanical performances are found to be attributed to the hierarchical structure of the PA gels, consisting of reversible ionic bonds at the 1 nm scale, permanent polymer network at the 10 nm scale, and bicontinuous phase network at the hundred nm scale. In this work, we systematically studied the phase network formation of these gels, aiming to answer the following three questions: (1) how the phase separation occurs? (2) what determines the phase structure? and (3) is this structure in thermal dynamically equilibrium or not? Our results show that, the phase separation occurs during dialysis of counterions from the gels and it is driven by the Coulombic and hydrophobic

interactions. The phase size d_0 and the number of aggregated chains in a unit cell of phase structure n scale with the molecular weight of partial chain between permanent effective crosslinking M_{eff} as $d_0 \sim M_{eff}$ and $n \sim M_{eff}^2$, respectively. Chemical crosslinker and topological entanglement suppress phase separation while hydrophobic interaction favors phase separation. An intrinsic correlation between the polymer density difference ($\Delta\rho$) between two phases and d_0 is observed, $\Delta\rho \sim d_0^2$, as a result of the competition between the driving force to induce phase separation and the resistance to suppress the phase separation. The phase separated structure is metastable, which is locally trapped by strong intermolecular interactions.

INTRODUCTION

Hydrogels, composed of three-dimensional polymer network and abundance of water, are a typical of soft and wet materials. The soft and wet nature of hydrogels make them broadly applicable to many fields, such as tissue engineering[1], drug delivery[2,3], sensors[4,5] and soft electronics[6,7]. Conventional hydrogels are mechanically brittle and weak, which limit their application severely. In the past decade, various mechanically strong and tough hydrogels were developed by using sacrificial bond strategy[8–12]. Sacrificial bonds break preferentially during deformation, dissipating energy and endowing the material a high toughness. Sacrificial bonds can be either chemical or physical bonds. Accordingly, these hydrogels can be categorized into two groups. One is double-network hydrogels (DN gel) with chemical bonds as sacrificial bonds[8,13–15]. Another is supramolecular hydrogels with physical bonds as sacrificial bonds[10,11,16–19]. As the breaking of chemical bonds is irreversible, DN gel softens permanently after deformation. In contrast, physical hydrogels can be fully recovery, even after large deformation, due to the reversible nature of physical bonds. Consequently, physical hydrogels have drawn great attention in recent years.

Past efforts on physical hydrogels mainly focused on developing new gel systems[20,21], studying their time-dependent behavior[22–27] and self-healing mechanism[28,29], while less attention was paid on the structure of these materials[30,31]. Due to the existence of physical interaction, polymer chains may locally aggregate to form heterogeneous structure. Recently, we found a series of self-healing and tough polyampholyte hydrogels have a hierarchical structure, consisting of reversible ionic bonds at the 1 nm scale, permanent polymer network at the 10 nm scale, and bicontinuous phase network at the hundred nm scale[31]. The bicontinuous phase separated structure consists of a soft phase network and a hard phase network, due to the

difference in polymer density. This structure is critical for the toughness and fatigue resistance of PA gels, as demonstrated by the recent uniaxial loading[31] and fatigue loading experiments[32].

The role of phase separated structure on toughness of PA gels was revealed in uniaxial loading experiment.[31] Upon loading, the bicontinuous phase network first shows a large affine deformation, during which the nanoscale chain conformation changes with ionic bond breaking to dissipate energy. At a certain large deformation, the strands of hard phase network start to rupture, and the load is transferred to the soft phase network. The soft phase network sustains the load, which effectively reduces stress concentration and prevents the catastrophic crack propagation. Upon further increasing the deformation, the soft phase finally ruptures and leads to the global failure of gel. Such a multi-scale rupture process dissipates significant amount of energy and gives a high toughness of PA gels. The role of phase separated structure on the fatigue resistance was revealed in a cyclic loading experiment.[32] Upon cyclic loading, the bicontiunous phase network orientates along stretching direction to induce a pronounced crack blunting and crack deceleration effect, resulting in an extremely slow crack growth even above the energy release threshold. The relative strength of soft and hard phases has also been demonstrated to be important for the mechanical behavior of PA gels[33].

Although the extremely important role of phase separated structure on mechanical performance of PA hydrogels, less is known on the structure formation mechanism. To understand the structure formation mechanism, we need to answer the following three questions: (1) how phase separation occurs? (2) what determines the phase structure?

and (3) is this structure in thermal dynamically equilibrium or not? For this purpose, we combined ultra-small- and small-angle X-ray scattering (USAXS and SAXS) to reveal the structure evolution during dialysis process of PA gels. In addition, the effects of chemical crosslinker concentration, monomer concentration at preparation, charge fraction and chemical structure of monomers on phase structure were studied. To check whether the phase separated structure is in thermal dynamically equilibrium or not, the effects of dialysis conditions on phase structure and the structure recovery of gel after experiencing salt solution were examined.

EXPERIMENTAL SECTION

Materials. Anionic monomer sodium p-styrenesulfonate (NaSS), cationic monomer 3-(methacryloylamino) propyl-trimethylammonium chloride (MPTC), UV initiator α-ketoglutaric acid (α-keto), chemical cross-linker N,N'-methylene-bis-acrylamide (MBAA) and sodium chloride (NaCl) were provided by Wako Pure Chemical Industries, Ltd., Japan. Cationic monomer methyl chloride quarternised N,N-dimethylamino ethylacrylate chloride (DMAEA-Q) was provided by MT AquaPolymer, Inc., Japan. The structure of chemicals is shown in Figure 1a. All chemicals were used as received and Millipore deionized water was used in all experiments.

Synthesis of PA hydrogels. Gels were prepared by one-step random copolymerization of positive and negative monomers at a high concentration, with or without chemical crosslinker. Cationic monomer, anionic monomer, UV initiator, and chemical crosslinker were dissolved in water at 50 ^{o}C to form a homogeneous precursor solution. The precursor solution was injected into a reaction cell consisting of a pair of glass plates separated by a silicone spacer of 2 mm-thick and was irradiated with 365

nm UV light in an argon atmosphere for 11 h. The obtained gel at this stage is named as as-prepared gel.

The as-prepared gels were dialyzed in three ways. The first is that, the as-prepared gels were dialyzed in water by submerging the gels in large amount of pure water at room temperature longer than one week, during which the counterions were removed and the gels reached equilibrium. The second is that, the as-prepared gels were dialyzed in pure water at a prescribed dialysis temperature until equilibrium, varied from 5 to 80 °C. Then, the gels were storage in pure water at room temperature for one week before measurement. The third is that, the as-prepared gels were dialyzed by two steps at room temperature: first in NaCl aqueous solution of prescribed concentration C_{NaCl} until equilibrium, and then in pure water for one week before measurement. Most of gels used in this work were dialyzed by the first way, and the gels dialyzed by the second and third ways were only used in studying the effect of dialysis conditions on phase structure.

Hereafter, we use the code P(NaSS-co-MPTC)-C_m-C_{MBAA} to denote the gels made from ionic monomers NaSS and MPTC and P(NaSS-co-DMAEA-Q)-C_m-C_{MBAA} to denote the gels made from ionic monomers NaSS and DMAEA-Q, where C_m (M) denotes the total monomer concentration at preparation and C_{MBAA} (mol%) denotes the crosslinker concentration in relative to C_m. In preparing all hydrogels, the concentration of initiator, $C_{\alpha\text{-keto}}$, is fixed at 0.1 mol% relative to C_m. The molar fraction of the anionic monomer NaSS in feed (anion charge fraction, f) is 0.525 for P(NaSS-co-MPTC) system and 0.515 for P(NaSS-co-DMAEA-Q) system, without special mention. Gels prepared at these charge fractions in feed have balanced charges in polymers.

Water content measurement. The water content c_w of a gel was measured with an electronic moisture device. The wet gel was first weight at room temperature and then heated to 120 ^oC to remove all water. Finally, the dry gel was cooled to room temperature and weight again. The water content c_w is calculated by $c_w = (m_0-m)/m_0$, where m_0 and m are the weight of initial wet gel and final dry gel, respectively. The polymer volume fraction ϕ_p of gel was calculated from the relation $\phi_p^{-1} = 1 + \rho_p c_w/\rho_w(1 - c_w)$, where $\rho_p = 1.19$ g/cm^3 and $\rho_w = 0.98$ g/cm^3 are the densities of PA and water, respectively.[27]

USAXS and SAXS measurements. The USAXS measurement was performed in BL20XU beamline, SPring-8, Japan. The energy of X-ray was 23 keV and the sample-to-detector distance was 160.5 m. A Pilatus 100 K detector was used, and the data acquisition time was 30 s per frame. The resolution of detector is 487 × 195 pixels with pixel size of 172 × 172 μm^2. Part of SAXS measurements was performed in BL05XU beamline, SPring-8, Japan. The energy of X-ray was 12 keV and the sample-to-detector distance was 3829.2 mm. A Pilatus 1 M detector was used, and the data acquisition time was 1 s per frame. The resolution of detector is 981 × 103 pixels with pixel size of 172 × 172 μm^2. Part of SAXS measurements was performed at the BL19U2 beamline, NCPSS, Shanghai, China. The sample-to-detector distance was 6225.6 mm. The energy of X-ray, the detector and the data acquisition time were the same as that in BL05XU beamline. The 2D SAXS patterns were analyzed with a Fit 2D software from European Synchrotron Radiation Facility[34]. All the SAXS data were corrected for X-ray beam fluctuation, detector spatial distortion, and background scattering.

Rheology measurements. Linear dynamic rheology measurements were carried out with an ARES rheometer (Rheometric Scientific Inc.). Disk shape samples with diameter of 15 mm were glued between two plates and surrounded by water during measurement. The autostrain function and gap adjustment were used to minimize compression on the sample. Frequency sweep measurement ranging from 0.1 to 100 rad/s were performed at different temperatures. During measurement, the temperature was increased stepwise from low to high and the shear strain was 0.1%. Before each measurement, the sample was kept at the set temperature for 5 min to reach equilibrium. The dynamic moduli taken at different temperatures were superimposed into a master curve with horizontal shift factor a_T and vertical shift factor b_T at a reference temperature of 24 °C, using the time-temperature principle (TTS).

RESULTS AND DISCUSSION

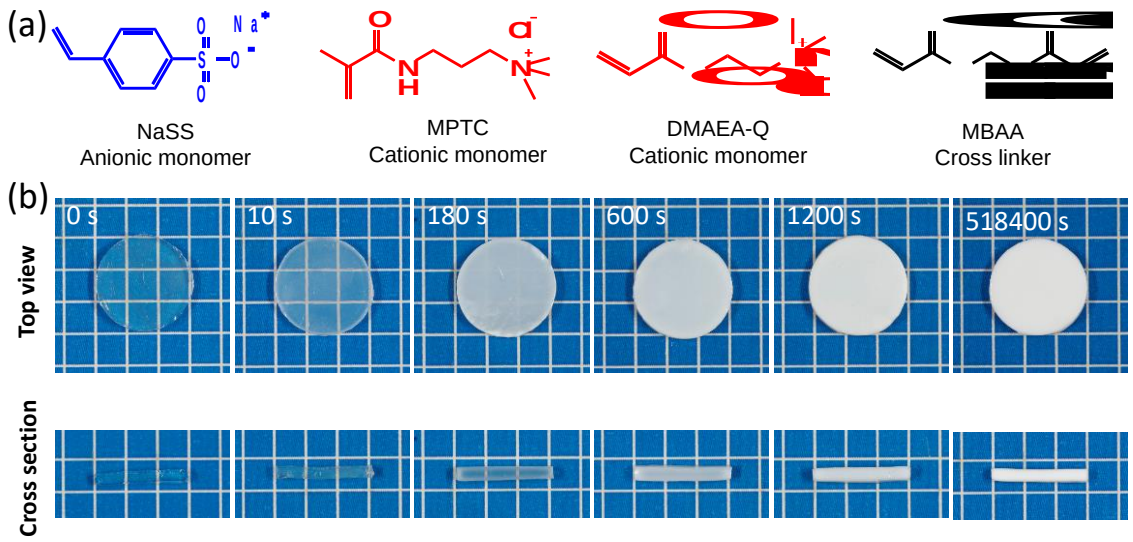

Figure 1. (a) Structure of the chemicals used for synthesizing PA gels. (b) Appearance of PA gels during dialysis in pure water at room temperature. The numbers in the images are the elapsed time after submerging the sample in pure water. The upper images show the top view of gels and the lower images show the cut cross section. The sample is P(NaSS-co-MPTC)-2.1-0. The mesh size of background lattice is 5 mm.

1. How phase separation occurs?

To investigate how phase separation occurs, we started from the as-prepared gel and measured the structure evolution during dialysis process of counterions. A PA gel, P(NaSS-co-MPTC)-2.1-0, was chosen as an example. The gel with this formulation has high toughness. The gel was dialyzed in pure water at room temperature. Figure 1b shows the optical images at different dialysis time. The as-prepared gel is semi-transparent (t = 0 s), implying that structure heterogeneity has already existed in the as-prepared gel. By dialyzing in water (t = 10 s), the turbidity of gel increases, suggesting an increase in the structure heterogeneity. Further increasing the dialysis time (t = 180 s), the appearance of gel changes to opaque white. Cut cross-sectional images show that the change of turbidity starts from the surface layers of the sample, suggesting that it is related to the diffusion of counterions from the gel to the water bath. The gel becomes

totally opaque white at the dialysis time of 1200 s. After that, no obvious change is observed in the optical image, up to dialysis equilibrium of the gel.

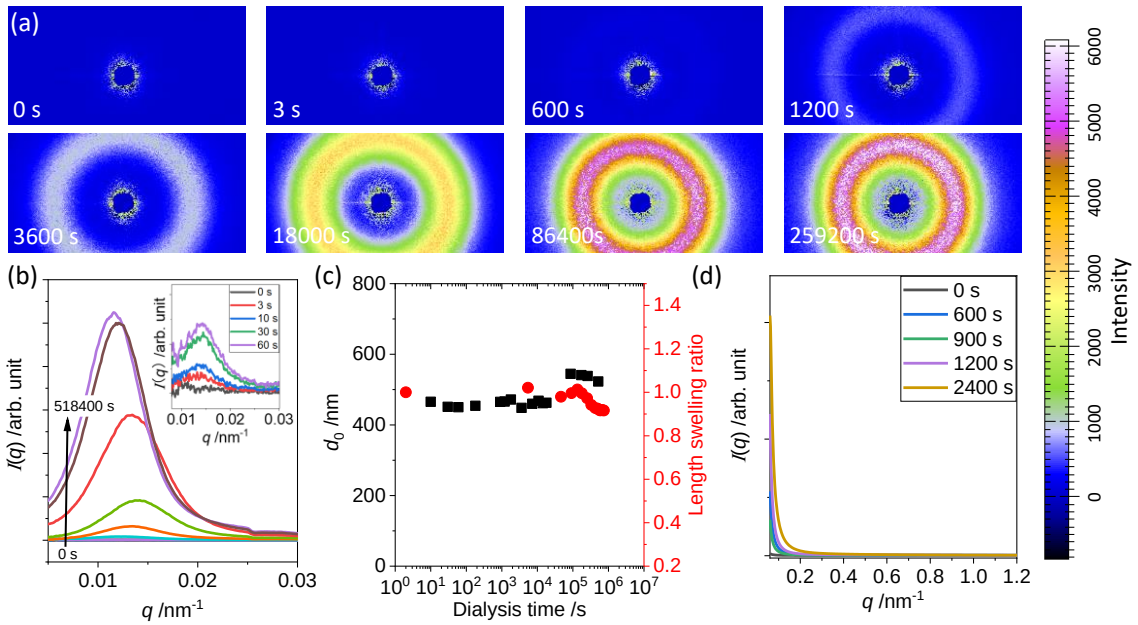

Figure 2. Structure evolution of PA gel during dialysis in pure water at room temperature. (a) 2D USAXS scattering patterns and (b) 1D scattering intensity profiles at several representative dialysis time. Inset in (b) shows the enlarged view of 1D scattering profiles in the initial stage of dialysis. (c) *d*-spacing and length swelling ratio (in relative to the as-prepared gel) change with dialysis time. The length swelling ratio change during dialysis was calculated with length change data taken from Cui et al.[25], where the gel with the same chemical composition and dialysis condition was used. (d) 1D SAXS profiles at several representative dialysis time. The sample is P(NaSS-co-MPTC)-2.1-0.

To reveal the phase structure formation behind the turbidity change, a combination of USAXS and SAXS, with a capability to detect structural length from 5 to 2710 nm, was used to measure the structure change during dialysis of the same gel at the same experimental conditions. For the as-prepared gel (t = 0 s), both the USAXS and SAXS show typical amorphous-like scattering (Figures 2), suggesting the absence of ordered structure in the measurement length scale. By dialysis, a scattering ring appears in 2D USAXS pattern immediately, and its intensity increases with dialysis time. This

scattering ring arises from the formation of phase separated structure, which gives the opaque appearance of gels in Figure 1b.

The 2D scattering patterns were radially averaged to obtain the q dependence of scattering intensity $I(q)$, where q is modulus of scattering vector. As shown in Figure 2b, even at the dialysis time of 3 s, a weak but clear correlation peak appears in $I(q) \sim q$ plot, suggesting the formation of well-organized phase separated structure. The peak intensity increases with increasing dialysis time, accompanying with a slight vibration in peak position. From the 1D scattering intensity profiles, we identified the peak position (q_{peak}) and computed the d-spacing (d_0) between adjacent soft regions or hard regions, based on the relation $d_0 = 2\pi/q_{peak}$. d_0 keeps almost constant with dialysis time (~ 500 nm), consistent with the small change in swelling ratio of gel during dialysis (Figure 2c). Note that the data of swelling ratio of sample during dialysis is from a previous result of the gel with the same chemical composition and dialysis condition.[25] A weak but sudden increase in d_0 appears at about 10^5 s, possibly from the phase coarsening.

Based on the above optical, USAXS and SAXS results, we discuss the structure evolution of PA gel during dialysis process. The as-prepared gel already has structure heterogeneity, as demonstrated by the semi-transparent appearance of gel. While at this stage, the structure is not well organized, and the heterogeneity is low, as demonstrated by the absence of correlation peak and weak scattering intensity in both SAXS and USAXS. This heterogeneous structure is possibly due to the non-evenly distributed weak and strong ionic bonds or/and entanglements in as-prepared gels. Our previous study showed that some strong inter-chain ionic bonds exist in the as-prepared gel[27].

These strong ionic bonds are believed to be formed around topological entanglements, due to the existence of a large amounts of counterions in the as-prepared gel.

Once being immersed in water for dialysis, the removing of counter-ions from gel substantially enhances the ionic bonds formation, both in inter-chains and intra-chains. As the polymer backbone is hydrophobic and the ionic side groups are hydrophilic, the ionic bond formation of the polymer chains significantly favors the aggregation of the hydrophobic polymer backbones. As a result, phase separation occurs. The phase separation starts from the surface of gel (Figure 1b), which is a clear evidence that the phase separation is initiated by the removement of counterions and the consequent ionic bond formation. The opaque surface layer becomes thicker and thicker by increasing dialysis time, suggesting that the content of phase separated structure increases with dialysis time. The time for gel becomes totally opaque is about 1200 s, which is much shorter than the time for the gel to reach dialysis equilibrium (about 1 week[25]). This suggests that the phase structure undergoes a reorganization process after its formation. The chain segments may locally adjust themselves to release the stress arising from phase separation process, which reduces internal stress concentration of the gel and helps to form more ionic bonds.

2. What determines the phase structure?

To study the factors that determine the phase structure, we systematically changed the compositions of PA gels, including chemical crosslinker concentration (C_{MBAA}), monomer concentration at preparation (C_m), anion charge fraction (f) and chemical structure of monomers, and measured their phase structure. All gels used in this section

were dialyzed in pure water at room temperature and the structure was measured after reaching dialysis equilibrium.

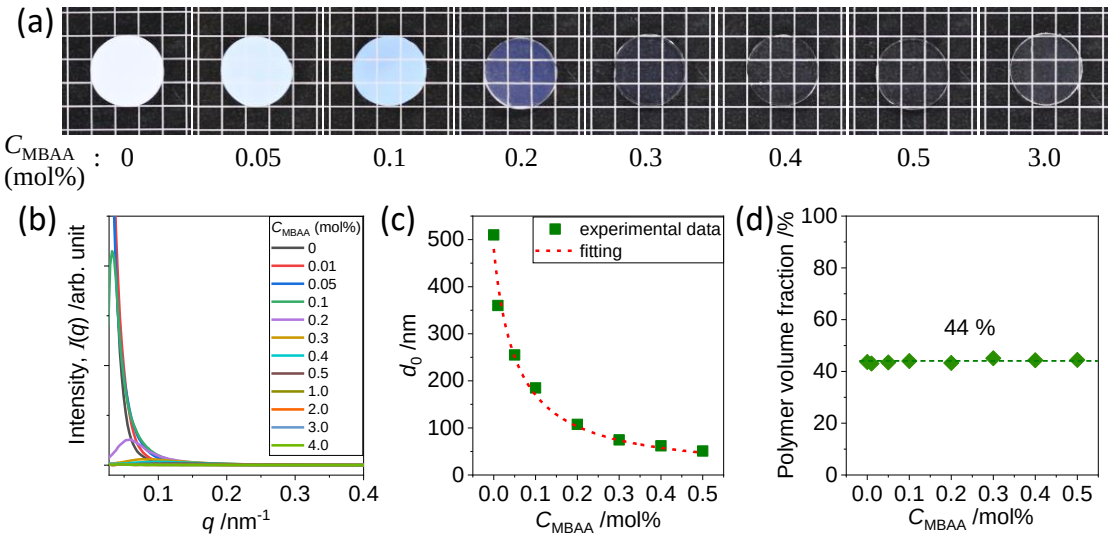

Figure 3. Effect of chemical crosslinker on the phase structure of PA gels. (a) Optical images, (b) 1D SAXS profiles, (c) *d*-spacing and (d) polymer volume fraction of gels at different chemical crosslinker concentrations. In (c), gels with *d*-spacing above 200 nm were measured by USAXS, while below that were measured by SAXS. The red fitting curve was obtained from the Equation (1) using k = 26.3 nm·mol% and C_e= 0.055 mol% as fitting parameters. The gel system is P(NaSS-co-MPTC)-2.1-C_{MBAA}. The mesh size of background lattice in (a) is 5 mm.

Effect of chemical crosslinker. Figure 3 shows the effect of chemical crosslinker on phase structure of PA gels, with P(NaSS-co-MPTC)-2.1-C_{MBAA} system as an example. The gel without chemical crosslinker (C_{MBAA} = 0 mol%) is opaque white (Figure 3a). By increasing chemical crosslinker concentration C_{MBAA} to 0.1 and 0.2 mol%, the gels become blue and purple, respectively. Further increasing C_{MBAA} to 0.3 mol% and more, the gels become fully transparent. The change in appearance of the gels suggests the structure change by increasing chemical crosslinker.

Figure 3b presents the 1D SAXS profiles of gels with different C_{MBAA}, which gives us two information. One is that, the peak position of correlation peak shifts to larger q

with increasing C_{MBAA}, suggesting a decrease in d_0 of the phase structure. d_0 decreases from about 510 to 40 nm, by increasing C_{MBAA} from 0 to 0.5 mol% (Figure 3c), which explains the appearance change of the gels. Another is that, the peak intensity decreases with increasing C_{MBAA}. The peak intensity is proportional to the contrast between two phases of the phase structure. Therefore, the phase contrast, or the difference in polymer density between soft and hard phases, becomes smaller with increasing chemical crosslinker. When C_{MBAA} is larger than 0.5 mol%, no correlation peak is observed, suggesting the disappearance of phase separation. Therefore, the chemical crosslinker suppresses phase separation, through decreasing the structure length and the phase contrast. When C_{MBAA} is larger a critical value, which is 0.5 mol% for this gel system, the gel becomes homogeneous and no phase contrast exists.

As mentioned above, the phase separation is due to the aggregation of hydrophobic polymer backbones. Adding chemical crosslinker can effectively suppress chain mobility and thus suppress phase separation. Since the PA gel is synthesized by random copolymerization of cationic monomer and anionic monomer at a high concentration, the polymers obtained in gels contain large amount of topological entanglements, which also serve as permanent effective crosslinking.[27] If d_0 is inversely related to the effective crosslinking density, it should follow the relationship

$$d_0 = k/(C_{MBAA} + C_e), \quad (1)$$

Here k is a prefactor and C_e is the crosslinking concentration caused by trapped topological entanglements. As the polymer volume fractions of these gels are almost same for C_{MBAA} ranging from 0 to 0.5 mol% (Figure 3d), we can assume C_e as a constant for the samples prepared from the same total monomer concentration C_m but

different chemical crosslinker concentration C_{MBAA} in the Equation 1. As shown in Figure 3c, using C_e = 0.055 mol% as a fitting parameter, a very good fitting to the *d*-spacing change is obtained, demonstrating that d_0 is indeed inversely proportional to the effective crosslinking density. This indicates that d_0 is linearly related to the effective molecular weight between the effective crosslinking points, M_{eff}. The constant polymer volume fraction, independent of the effective crosslinking density, indicates that the partial chains take the collapsed globule conformation in these PA gels.[35]

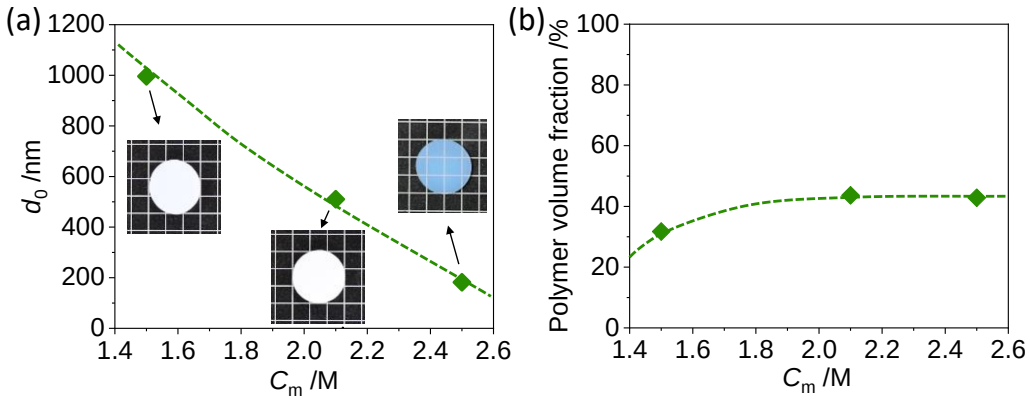

Figure 4. Effect of monomer concentration at preparation on phase structure of PA gels. (a) *d*-spacing and (b) polymer volume fraction of equilibrated gels synthesized at different total monomer concentration C_m. Insets in (a) show the optical images of gels and the mesh size of background lattice is 5 mm. d_0 of gels with C_m of 1.5 M and 2.1 M were measured by USAXS, and d_0 of gel with C_m of 2.5 M was measured by SAXS. The gel system is P(NaSS-co-MPTC)-C_m-0.

Effect of monomer concentration at preparation. Our previous study have shown that the PA gels prepared at high monomer concentrations C_m are deswelling, while the gels prepared at low C_m are swelling, compared to their as-prepared states.[11,36] Here we focus on the effect of C_m on phase structure of gels prepared at high C_m. If the overall molecular weight does not change with the monomer concentration, larger C_m brings more topological entanglements, as predicted by the theoretical relation $C_e \sim C_m^{2.3}$.[35] Figure 4a presents the change of optical appearance and d_0 with increasing C_m, with

P(NaSS-co-MPTC)-C_m-0 system as an example. The gel with C_m of 1.5 M has a d_0 of about 1000 nm, while d_0 decreases to about 180 nm when increasing C_m to 2.5 M. Meanwhile, the gels change from opaque white to blue appearance with increasing C_m , due to the decreasing in d_0, similar to the effect of increasing chemical crosslinker. As the number of topological entanglements increases with increasing C_m and it does not change during dialysis, the gels prepared at higher C_m have more topological entanglements[27]. These topological entanglements act as permanent effective crosslinkers, suppress the phase separation through decreasing *d*-spacing and phase contrast, and play the role like by chemical crosslinkers. As *d*-spacing changes in a quite large range, a combination of USAXS and SAXS was used to measure d_0 of these gels, which brings difficulty to compare their peak intensities and phase contrasts. In addition, the polymer volume fractions of these gel increases slightly from about 32 to 43 % by increasing C_m from 1.5 M to 2.5 M (Figure 4b).

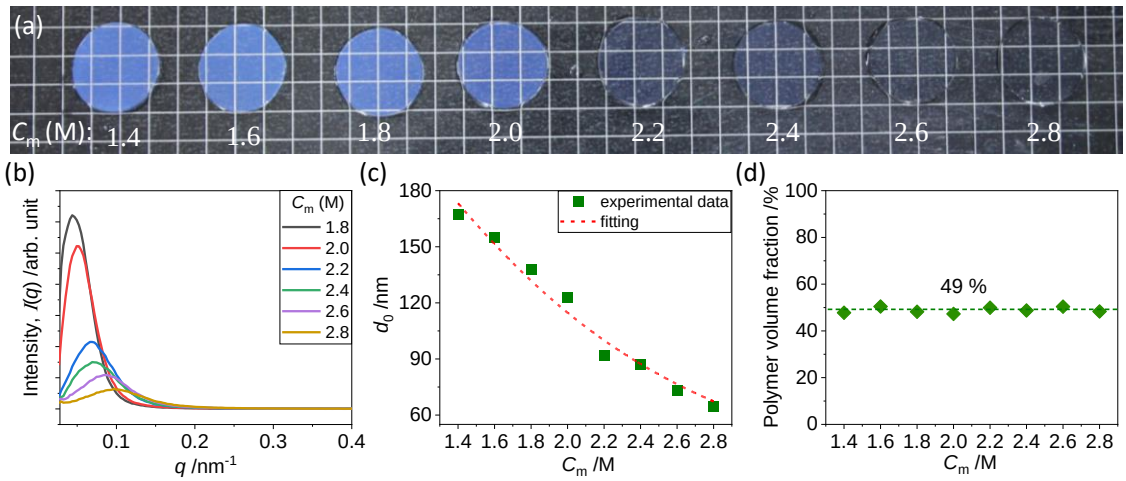

Figure 5. Effect of total monomer concentration at preparation on phase structure of PA gels. (a) Optical images, (b) 1D SAXS profiles, (c) *d*-spacing and (d) polymer volume fraction of equilibrated gels synthesized at different monomer concentrations. The red fitting curve in (c) was obtained from the Equation (2) using k = 28.9 nm·mol% and α = 0.031 mol%·M$^{-2.3}$ as fitting parameters. All d_0 were measured by SAXS. The mesh size of background lattice in (a) is 5 mm. The gel system is P(NaSS-co-DMAEA-Q)-C_m-0.1.

Fortunately, in another gel system, P(NaSS-co-DMAEA-Q)-C_m-0.1, d-spacing falls into the measurement range of SAXS (Figures 5b and 5c). At the same time, polymer volume fractions of these gels are almost same (around 49 %), in the studied C_m ranging from 1.4 to 2.8 M (Figure 5d). As shown in Figures 5, with increasing C_m, the appearance of gels changes from blue to transparent, accompanying with a decrease of d_0 from 167 to 65 nm. Meanwhile, the peak intensity in scattering profiles also dramatically decreases with increasing C_m, suggesting a decrease of the contrast between two phases. This result clearly demonstrates that the topological entanglements also suppress the phase separation, as like the chemical crosslinkers. Since $C_e \sim C_m^{2.3}$, we put $C_e = \alpha C_m^{2.3}$ into Equation 1 and the equation becomes

$$d_0 = k/(C_{MBAA} + \alpha C_m^{2.3}), \quad (2)$$

We fitted the d-spacing change data with Equation 2 using fitting parameter k = 28.9 nm·mol% and α = 0.031 mol%·$M^{-2.3}$. As shown in Figure 5c, a very good fitting to the d-spacing change is obtained, further demonstrating that the decrease in d_0 with C_m is due to the increase in topological entanglements.

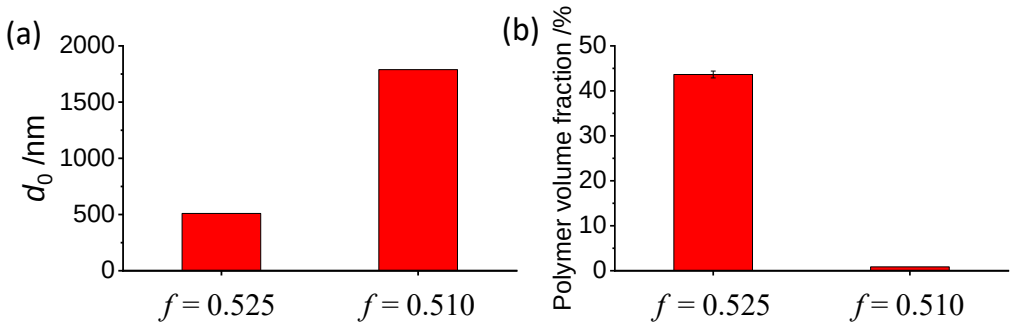

Figure 6. Effect of anion charge fraction on phase structure of PA gels. Two charge fractions in feed were used, one is f = 0.525 that results in a gel at the charge balanced point, another is f = 0.510 that results in a gel with slightly excess of cation charge. (a) d-spacing and (b) polymer volume fractions of these two gels. d_0 was measured by USAXS. The gel system is P(NaSS-co-MPTC)-2.1-0.

Effect of anion charge fraction. PA gels with balanced or near balanced charges shrink, while gels with unbalanced charges swell, compared to their as-prepared states.[11] Therefore, it is expected that the phase structure also depends on the charge ratio. Figure 6 gives an example, P(NaSS-co-MPTC)-2.1-0%, to show the effect of charge ratio on the phase structure. For the gel with balanced charges (f = 0.525 in feed), d_0 is about 510 nm. For the gel with slightly excess of cations (f = 0.510 in feed), d_0 increases to about 1800 nm. The polymer volume fractions of these two gels are also significantly different. For the gel with f = 0.525, the polymer volume fraction is around 44 %, while it decreases to 1 % for the gel with f = 0.510. This result is easy to understand, because at charge balanced point, all the small counter ions were removed from the gel. Coulomb and hydrophobic attractions prevail and the polymer chains collapse, leading to the deswelling of gel and thus high polymer volume fraction. While at charge unbalanced point, the counterions of unbalanced polyions generate a large osmotic pressure, which favors the swelling. During the swelling, both the soft and hard phases swell, giving a larger d_0. As the USAXS data of these two samples were measured at different time, it is not easy to compare their peak intensity and phase contrast directly. But it is expected that the phase contrast of the swollen gel is much larger than the shrunken gel, as the soft phase is weaker and easier to swell than the hard phase.

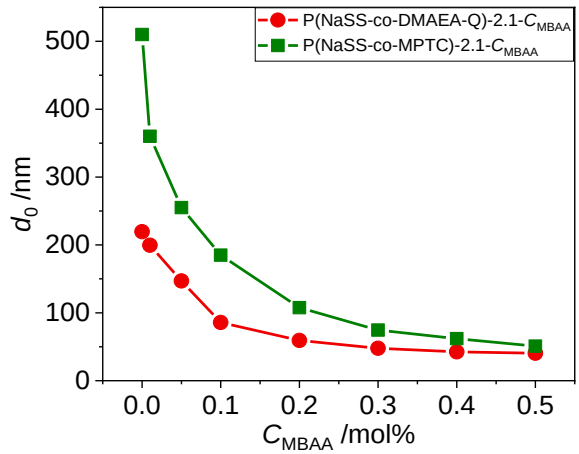

Figure 7. Effect of chemical structure of monomers on phase structure of PA hydrogels. *d*-spacing change as a function of chemical crosslinker concentration for two gel systems, P(NaSS-co-DMAEA-Q)-2.1-C_{MBAA} and P(NaSS-co-MPTC)-2.1-C_{MBAA}. d_0 of P(NaSS-co-DMAEA-Q)-2.1-C_{MBAA} system was measured by SAXS. d_0 of P(NaSS-co-MPTC)-2.1-C_{MBAA} system above 200 nm was measured by USAXS while below was measured by SAXS.

Effect of chemical structure of monomers. The chemical structure of monomers plays an important role in phase structure of PA gel. Figure 7 compares *d*-spacing of two gel systems with the same anionic monomer NaSS but different cationic monomers of MPTC and DMAEA-Q. These two gel systems were prepared at the same C_m and have almost same polymer volume fraction. First, we compare the phase structure for two gels without chemical crosslinker, P(NaSS-co-MPTC)-2.1-0 and P(NaSS-co-DMAEA-Q)-2.1-0. d_0 of P(NaSS-co-MPTC)-2.1-0 gel is about 510 nm, which is much larger than d_0 = 219 nm of P(NaSS-co-DMAEA-Q)-2.1-0 gel. This difference is expected to come from the difference in the hydrophobicity of MPTC and DMAEA-Q monomers. The hydrophobicity of MPTC is larger than that of DMAEA-Q. As the phase separation of PA gel is due to the aggregation of hydrophobic polymer backbones, the larger hydrophobicity of monomer, the stronger aggregation of polymer backbones and thus the larger *d*-spacing.

For both two gel systems, d_0 decreases with increasing C_{MBAA}. At the same time, the difference in d_0 between them becomes smaller. When C_{MBAA} reaches to 0.5 mol%, d_0 of them are almost same, which are 51 and 41 nm, respectively, for gels with MPTC and DEAEA-Q monomers. These results suggest that, both the chemical crosslinker and the hydrophobicity influence the phase separation of PA gels, but they work in an opposite way. At low chemical crosslinker concentration, hydrophobic interaction dominates the phase structure. So, the gel with more hydrophobic monomer has a much larger d_0. At high chemical crosslinker concentration, chemical crosslinker dominates the phase structure. Therefore, d_0 for two gels system are almost same.

3. Is the phase separated structure in thermal dynamically equilibrium or not?

To check whether the phase separated structure is in thermal dynamically equilibrium or not, we adopted two methods. One is to change the dialysis kinetics for as-prepared gel, either by dialyzing the sample first in NaCl solution and then in water or by changing the dialysis temperature. Another is to change the thermodynamic environment of equilibrated gel and then move the gel back to the original thermodynamic environment. In case that the phase separated structure is in thermodynamic equilibrium state, it should not depend on the history it is formed, and it should recover to the original state after a disturbance of thermodynamic environment. In case that the phase separated structure is in non-equilibrium state, it should depend on the history it is formed, it may not recover to the original state after a disturbance of thermodynamic environment. In this part, P(NaSS-co-DMAEA-Q)-2.6-0.1 gel was used as an example.

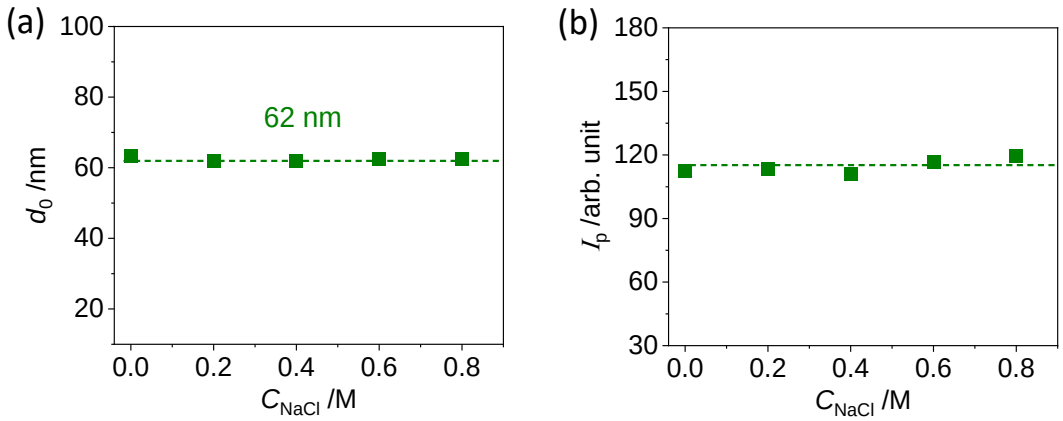

Figure 8. Effect of dialysis kinetics on phase structure of PA gel. The as-prepared gels were first dialyzed in NaCl solutions of prescribed concentrations (C_{NaCl}) at room temperature for one week, and then were dialyzed in pure water for another week. After that, SAXS was used to measure the phase structure of these gels. (a) *d*-spacing and (b) peak intensity of the gels against the NaCl concentration of dialysis solution. The gel is P(NaSS-co-DMAEA-Q)-2.6-0.1.

Effect of dialysis kinetics. In this experiment, the as-prepared gels were dialyzed by two steps, first in NaCl solution, and then in water. By changing the NaCl concentration (C_{NaCl}) in the dialysis solution, the dialysis kinetics of counterions (Na^+ and Cl^-) from gels are different. The dialysis kinetics depends on the concentration difference of these ions inside and outside of the gel. The counterions in the as-prepared gel have an initial concentration that is half of the monomer concentration ($C_m/2$). For a bath solution with much larger volume than the gel, in the first step dialysis in C_{NaCl} solution, the maximum driving force for dialysis is proportional to ($C_m/2 - C_{NaCl}$), which decays with the progress of dialysis until the concentration difference becomes zero at equilibrium. In the second step of dialysis in water, the maximum driving force for dialysis is proportional to C_{NaCl}, which decays with the progress of dialysis until all the counter-ions are removed from the gel. Thus, by the two-step dialysis process, we can control the dialysis kinetics. The higher the NaCl concentration C_{NaCl}, the slower the dialysis kinetics of counterions from gel in the first step dialysis. A series of NaCl

aqueous solutions with C_{NaCl} = 0 ~ 0.8 M were used to dialyze the sample P(NaSS-co-DMAEA-Q)-2.6-0.1 that has C_m = 2.6 M. Figure 8 displays the *d*-spacing and peak intensity against the NaCl concentration. Both d_0 and peak intensity (I_p) do not change with C_{NaCl}, in the studied C_{NaCl} range, suggesting that the phase structure does not change with dialysis kinetics of counterions.

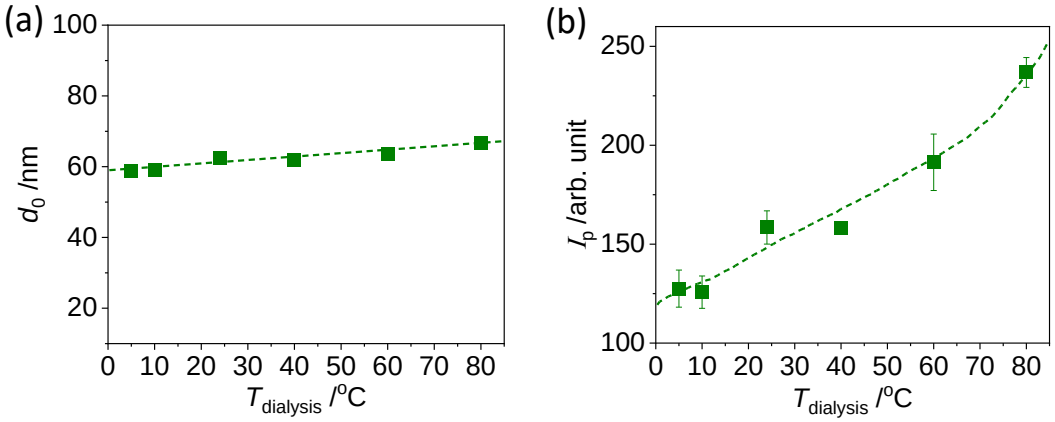

Figure 9. Effect of dialysis temperature on phase structure of PA gel. The as-prepared gels were dialyzed in pure water of different temperatures to reach equilibrium. Then the gels were moved to the pure water with room temperature for one week and measured with SAXS. (a) *d*-spacing and (b) peak intensity of gels as a function of dialysis temperature. The gel is P(NaSS-co-DMAEA-Q)-2.6-0.1.

Effect of dialysis temperature. In this experiment, the as-prepared gels were dialyzed in pure water under different temperatures ($T_{dialysis}$) to reach equilibrium, and then equilibrated in water at room temperature for one week. The time for reaching dialysis equilibrium depends on $T_{dialysis}$, which is about 1 day for $T_{dialysis}$ = 80 °C and more than 1 month for $T_{dialysis}$ = 5 °C. Figure 9 shows the *d*-spacing and peak intensity change as a function of dialysis temperature. d_0 increases slightly with $T_{dialysis}$, from 59 to 67 nm by increasing $T_{dialysis}$ from 5 to 80 °C (Figure 9a). At the same time, I_p also increases with $T_{dialysis}$, suggesting that the phase contrast also increases with dialysis temperature (Figure 9b). Since the dialysis kinetics does not influence the phase

structure as shown by Figure 8, this result indicates that hydrophobic interaction, which is entropy-driven, plays an important role to induce the phase separation.

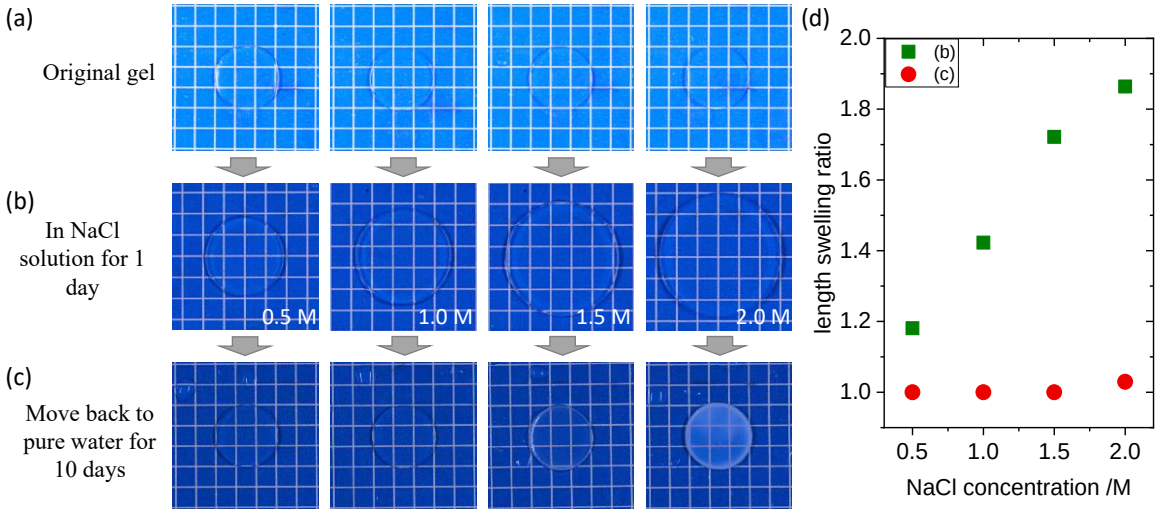

Figure 10. Structure reversibility of PA gel. The water-equilibrated gels were put in salt solutions with different NaCl concentrations for 1 day. Then the gels were moved to pure water for 10 days. (a-c) Photos to show the appearance of gel at different states, (a) original gel that equilibrated in water, (b) after immersing in NaCl solution for 1 day and (c) after moving back to pure water for 10 days. The numbers (b) present the NaCl concentration of salt solution. (d) Length swelling ratio of gels in (b) and (c), in relative to the original gels in (a), calculated from the diameter change of gels. The gel is P(NaSS-co-DMAEA-Q)-2.6-0.1. The mesh size of background lattice is 5 mm.

Disturbance of thermodynamic environment. To check whether the structure of gel can recover or not after experiencing a disturbance of thermodynamic environment, we put gels that initially being equilibrated in pure water at room temperature to NaCl solutions for 1 day, and then moved them back to pure water. The initially water-equilibrated gels are transparent, as shown in Figure 10a. After immersing in NaCl solution for one day, the transparency of gel keeps, while the size of gel increases (Figure 10b). Adding salts destroy ionic bonds, leading to the swelling of gel. The swelling degree increases with increasing NaCl concentration (Figure 10d). For example, the length swelling ratio of gel is about 120%, in relative to the original gel,

when NaCl concentration is 0.5 M, while it increases to about 190% when NaCl concentration is 2.0 M. After moving back to pure water for a certain time, all gels can recover to the original size, which should be attributed to the elasticity from chemical crosslinker (Figure 10c). While the recovery of appearance depends on the concentration of NaCl solution. At relatively low NaCl concentrations (0.5 M and 1.0 M), the gel recovers to transparent appearance, which is the same as the original gels. At relatively high NaCl concentrations (1.5 M and 2.0 M), the gels become opaque, significantly different to the originally transparent gel, even after a long recovery time of 10 days. The change in appearance suggests that the structure changes of gel after experiencing solution with high NaCl concentration.

Now we combine the results on dialysis conditions of as-prepared gel and disturbance of thermodynamic environment of equilibrated gel, to discuss the stability of the phase separated structure. The phase structure does not depend on NaCl concentration of dialysis solution, while depends on the dialysis temperature, suggesting that it is not in the stable or unstable state. Instead, it is in a metastable state. This argument is also supported by the results of disturbance of thermodynamic environment of equilibrated gel. The gel can fully recover to the initial state after experiencing a small or moderate disturbance of thermodynamic environment, but it cannot fully recover after experiencing a large disturbance of thermodynamic environment, suggesting that it locates in a local minimum in the free energy landscape. In other words, this structure is in a metastable state. This is easy to understand because in each PA chain positive charged monomers and negative charged monomers are randomly distributed along chain backbone. These charged monomers have both repulsion and attraction. Therefore, polymer chains cannot have a specific microstructure with

perfectly minimized interaction energy. Instead, they take many microstructures that locally have minimal energies.[37–39] This explain why the phase separated structure is metastable.

These results also suggest that although the phase separation is initiated by the removal of counterions, while the dialysis kinetics of counterions does not change the phase structure, as demonstrated by the same *d*-spacing and peak intensity of gels dialyzing under different NaCl solutions. The slight increase in *d*-spacing and phase contrast with dialysis temperature can be explained from the entropy effect of hydrophobic interaction. The phase separation is driven by aggregation of hydrophobic chain backbones. The hydrophobic interaction is entropy-driven, thus higher dialysis temperature results in stronger hydrophobic interaction, which induces higher density contrast between soft and hard phases, as well as slightly larger *d*-spacing. This argument is also supported by the fact that more hydrophobic monomers have larger *d*-spacing and higher phase contrast. The structure recovery of equilibrated gel after experiencing NaCl solution is probably related to the change of topological entanglements. The gel swells in NaCl solution and the swelling degree depends on NaCl concentration. A weak or moderate swelling does not destroy the topological entanglements, so the gel can be fully recoverable. While a strong swelling may destroy some topological entanglements, so the gel cannot be fully recoverable. Therefore, the topological entanglement or chemical crosslinker plays a role in remembering the phase structure.

4. Correlation between *d*-spacing and phase contrast.

All SAXS and USAXS results of PA gels show that the peak intensity or phase contrast increases with *d*-spacing, no matter such structure changes were obtained by different approaches, that is, by changing the monomer concentration at preparation, chemical crosslinker concentration or dialysis temperature of gels. Figure 11a summarize the peak intensity of equilibrated gels under various preparation conditions against *d*-spacing. It should be noted that it is meaningless to compare the scattering intensity between different sets of data, because the scattering intensity depends on many factors, such as incident beam intensity, exposure time and so on. Although theoretically it is possible to correct all these factors. However, in our experiments, different sets of samples were measured at different time and beam lines. Some information such as incident beam intensity was not provided by some beam lines. So here we just compare the scattering intensity within each set of data that obtained at the same time and the same beam line, where the influence of above factors is negligible. As shown in Figure 11a, all sets of data show similar trend of evolution of peak intensity I_p with *d*-spacing d_0. By shifting the data in Figure 11a vertically, all sets of data collapse into one master curve of $I_p \sim d_0^4$ (Figure 11b). This result indicates an intrinsic correlation between the size and the contrast of phase separated structure.

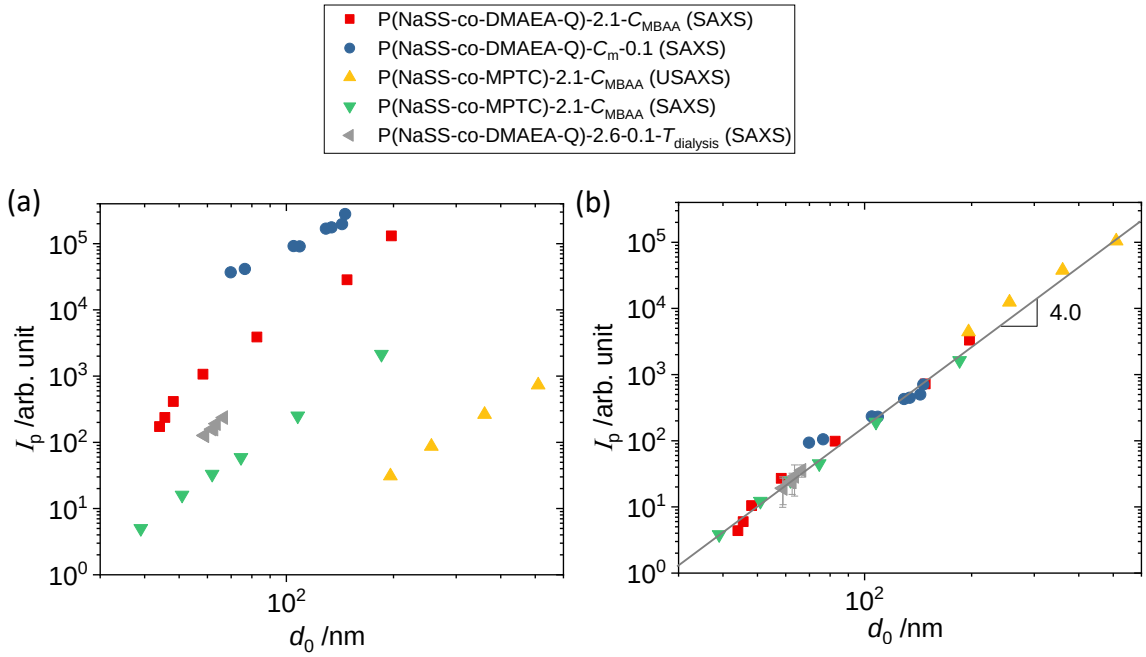

Figure 11. Correlation between peak intensity and *d*-spacing of equilibrated PA gels prepared with different monomers, monomer concentrations at preparation, chemical crosslinker concentrations and dialysis temperatures. (a) Relationship between peak intensity and *d*-spacing. (b) Master curve of peak intensity against *d*-spacing by vertically shifting the data in (a). Each set of data was marked with the same symbol and same color.

According to the scattering theory[41], the peak intensity I_p for a two-phase system is proportional to $v_1 v_2 (\Delta\rho)^2$, where v_1 is the volume fraction of phase 1, v_2 is the volume fraction of phase 2 and $\Delta\rho$ is the electron density difference between them. In case of PA gels studied here, v_1, v_2 and $\Delta\rho$ can be considered as the volume fractions of soft and hard phases, and their density difference, respectively. If we assume v_1 and v_2 do not change with preparation conditions of gel, a relationship of $\Delta\rho \sim d_0^2$ can be obtained. We think this assumption is reasonable, because $\Delta\rho$ definitely changes with the preparation conditions of gel, as demonstrated by the fact that at high crosslinker concentration the gel becomes homogeneous and no phase contrast exists. If v_1 and v_2

also change with preparation conditions, it is unlikely that all sets of data rightly collapse into one master curve of $I_p \sim d_0^4$. Qualitatively, it is easy to understand why there is a quantitative relationship between $\Delta\rho$ and d_0. A larger d-spacing means less constraint on fluctuation of polymer chain density, which leads to a larger phase contrast.

5. Correlation between the phase structure and the molecular structure.

The results in Figures 3 and 5 suggest that the size of phase structure (d_0) is linearly related to the molecular weight between the permanent effective crosslinking points, M_{eff}. Here, we discuss quantitatively the relation between d_0 and M_{eff}. Generally, M_{eff} can be related to the partial chain density v_e, by $M_{eff} = \phi_p\rho_p/v_e$, where ϕ_p and ρ_p are the polymer volume fraction and the polymer density of the gel, respectively. Although the partial chain density v_e in the hard phase and soft phase are different, for simplicity, here we discuss the average v_e. We estimate the average v_e by two methods. In the first method, we estimate v_e from the chemical composition. We assume that all the in feed crosslinkers and monomers were reacted to form the gel, then, $v_e = 2C_m(C_{MBAA} + \alpha C_m^{2.3})$, as ($C_{MBAA} + C_e$) is the crosslinker concentration in relative to C_m. The prefactor of 2 comes from the fact that a bifunctional crosslinker connects four partial chains together and each chain is shared by two crosslinkers. In the second method, we estimate v_e from the plateau shear modulus of the gels using the relation $G' = v_e kT$,[35] where k is Boltzmann constant and T is temperature. We take G' at the lowest measurement frequency around 10^{-6} s^{-1} as the plateau modulus arising from the permanent effective crosslinking, since at such a low frequency the contribution of ionic bonds to shear modulus is expected to be negligible (Figure 12 a-b).

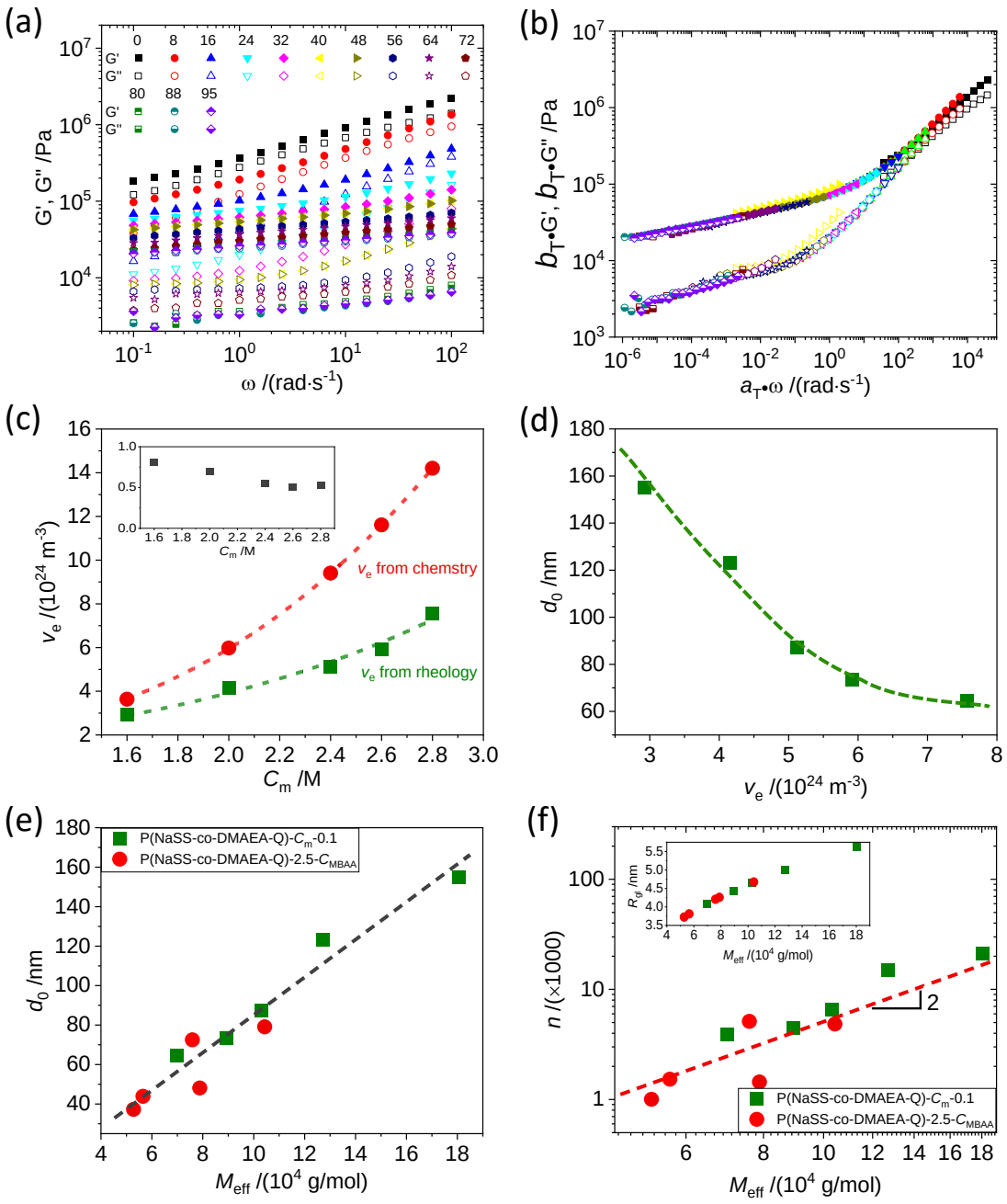

Figure 12. (a) linear viscoelastic data measured at different temperatures and (b) the constructed master curve for P(NaSS-co-DMAEA-Q)-2.8-0.1 gel. (c) Partial chain density, ν_e, calculated from the chemical composition and from the plateau shear modulus of rheology. Inset in (c) shows the ratio of ν_e calculated from shear modulus to ν_e calculated from chemical composition. (d, e) *d*-spacing, d_0, as a function of (d) ν_e and (e) molecular weight of partial chains, M_{eff}. (f) Number of aggregated chains, n, changes with M_{eff}. Inset in (f) shows the change of globule size with M_{eff}. The gel system used in (c, d) is P(NaSS-co-DMAEA-Q)-C_m-0.1. The gel systems used in (e, f) are P(NaSS-co-DMAEA-Q)-C_m-0.1 and P(NaSS-co-DMAEA-Q)-2.5-C_{MBAA}.

Figure 12c shows the ν_e determined from the rheology measurement and that calculated from the in-feed chemical composition, with P(NaSS-co-DMAEA-Q)-C_m-0.1 system as an example. We notice that the value of former deviates from the latter and the deviation increases with the increase of the monomer concentration. The deviation should come from the poor crosslinking reaction efficiency when the viscosity of the system becomes high. As shown previously, in the crosslinking reaction of a hydrogel, for some of the MBAA crosslinkers, only one of the two vinyl groups of a crosslinker is reacted and the other one is unreacted due to reduced mobility.[40] From the ratio of ν_e determined from the rheology measurement and that calculated from the in-feed chemical composition (Figure 12c, inset), the efficiency of chemical crosslinker decreased from 80 % to 50% with the increase of monomer concentration C_m from 1.6 M to 2.8 M. This result shows that using the in feed chemical composition to estimate the network structure contains large error. We adopt ν_e determined from the rheology measurement in the following discussion. The plot of d_0 as a function of ν_e is shown in Figure 12d. d_0 decreases with increasing ν_e. The effective molecular weight of a partial chain M_{eff} (g/mol) was also calculated with the relation $M_{eff} = \phi_p \rho_p / \nu_e$. Figure 12e presents d_0 as a function of M_{eff}, where a linear relation is observed for both P(NaSS-co-DMAEA-Q)-C_m-0.1 and P(NaSS-co-DMAEA-Q)-2.5-C_{MBAA} systems. This further demonstrates that d_0 is linearly related to M_{eff}, no matter M_{eff} is changed by chemical crosslinker or topological entanglement.

Next, we discuss the number of partial chains in a unit cell of mesoscale phase structure. The size of a partial chain in collapsed globule conformation, R_{gl}, is related to its effective molecular weight M_{eff} through the polymer volume fraction of the gel, $\phi_p \cong$

$(M_{eff}/M_0)d^2b/R_{gl}^3$, where M_0, d, and b are the average molecular weight of monomers, the effective monomer diameter, and the monomer length, respectively. Therefore, $R_{gl} \cong [(M_{eff}/M_0)d^2b/\phi_p]^{1/3}$, which show that $R_{gl} \sim M_{eff}^{1/3}$ for the collapsed globule chains. The exponent of 1/3 suggests a weak dependence of R_{gl} on M_{eff}. The number of partial chains in a phase unit of length d_0 can be roughly estimated by $n = (d_0/R_{gl})^3$. Since d_0 is linearly proportional to M_{eff}, we have $n \sim M_{eff}^2$, which means the aggregated number of partial chains in a phase cell strongly depends on the molecular weight of the partial chain. Here we take P(NaSS-co-DMAEA-Q)-C_m-0.1 and P(NaSS-co-DMAEA-Q)-2.5-C_{MBAA} gels as examples to quantitatively calculate n. From the molecular structure of the polymer, M_0 is 200 g/mol, d is about 0.8 nm and b is about 0.15 nm.[35] Using these parameters, R_{gl} increases only from about 3.7 to 5.6 nm by increasing M_{eff} from 5.3×10^4 to 1.8×10^5 (Figure 12f, inset). The n rapidly increases from about 1000 to 21000 with increase of M_{eff} from 5.3×10^4 to 1.8×10^5 (Figure 12f). These results demonstrate that the phase structure is formed by the aggregation of abundant of partial chains, the length size d_0 and the number of aggregated chains n scale with the molecular weight of partial chains M_{eff} as $d_0 \sim M_{eff}$ and $n \sim M_{eff}^2$, respectively.

From the dependences of the density difference between soft and hard phases $\Delta\rho$ with the phase size d_0, $\Delta\rho \sim d_0^2$, and d_0 with M_{eff}, $d_0 \sim M_{eff}$, we obtain $\Delta\rho \sim M_{eff}^2$. Given that $\Delta\rho$ is linearly related to the difference of polymer volume fraction between the two phases, it is still an open question why the overall polymer volume fraction ϕ_p of the PA gels is independent of M_{eff}. In addition, further studies are also required to explain quantitatively the universal relationship between $\Delta\rho$ and d_0 observed in this study.

CONCLUSION

In conclusion, we systematically studied the phase separation behavior of tough and self-healing PA hydrogels, including the structure evolution during dialysis, and the effects of monomer concentration at preparation, chemical crosslinker concentration, charge fraction and chemical structure of monomers on phase structure of the gels. In addition, the stability of phase separated structure was also examined. Our main conclusions are listed as follows: (1) the phase separation is initiated by the dialysis of counterions from as-prepared gels, while the dialysis kinetics of counterions does not influence the phase structure; (2) the phase structure is formed by the aggregation of abundant of partial chains, the phase size d_0 and the number of aggregated chains in a unit cell of phase structure n scale with the molecular weight of partial chains M_{eff} as $d_0 \sim M_{eff}$ and $n \sim M_{eff}^2$, respectively; (3) hydrophobic interaction is a driving force for phase separation, gels with more hydrophobic monomers have larger d-spacing and phase contrast ; (4) chemical crosslinker and topological entanglement suppress phase separation, by decreasing d-spacing and phase contrast; (5) the phase separated structure is metastable, which is locally trapped by strong intermolecular interactions; (6) the polymer density difference between two phases has an intrinsic correlation with structural length, $\Delta\rho \sim d_0^2$, due to the constraint effect of size on polymer density fluctuation. We believe these results are vital important for the fundamental understanding of hydrogels with abundant of physical interactions and benefit the design of new type of tough and self-healing materials with controlled phase separated structure.

ACKNOWLEDGMENTS

We thank Prof. Michael Rubenstein and Prof. Wei Hong for helpful discussion. This research was supported the Japan Society for the Promotion of Science (JSPS) KAKENHI (grant no. JP17H06144 and JP19K23617). The Institute for Chemical Reaction Design and Discovery (ICReDD) was established by World Premier International Research Initiative (WPI), MEXT, Japan. We thank the staffs from BL19U2 beamline of National Facility for Protein Science in Shanghai (NFPS) at Shanghai Synchrotron Radiation Facility, BL20XU and BL05XU beamlines from SPring-8, for assistance during data collection.

REFERENCES

(1) Lee, K. Y.; Mooney, D. J. Hydrogels for Tissue Engineering. *Chem. Rev.* **2001**, *101* (7), 1869–1880.

(2) Hoare, T. R.; Kohane, D. S. Hydrogels in Drug Delivery: Progress and Challenges. *Polymer (Guildf).* **2008**, *49* (8), 1993–2007.

(3) Kamath, K. R.; Park, K. Biodegradable Hydrogels in Drug Delivery. *Adv. Drug Deliv. Rev.* **1993**, *11* (1–2), 59–84.

(4) Haque, M. A.; Kurokawa, T.; Kamita, G.; Yue, Y.; Gong, J. P. Rapid and Reversible Tuning of Structural Color of a Hydrogel over the Entire Visible Spectrum by Mechanical Stimulation. *Chem. Mater.* **2011**, *23* (23), 5200–5207.

(5) Richter, A.; Paschew, G.; Klatt, S.; Lienig, J.; Arndt, K.-F.; Adler, H.-J. Review

on Hydrogel-Based PH Sensors and Microsensors. *Sensors* **2008**, *8* (1), 561–581.

(6) Yuk, H.; Lu, B.; Zhao, X. Hydrogel Bioelectronics. *Chem. Soc. Rev.* **2019**, *48* (6), 1642–1667.

(7) Zhao, Y.; Xuan, C.; Qian, X.; Alsaid, Y.; Hua, M.; Jin, L.; He, X. Soft Phototactic Swimmer Based on Self-Sustained Hydrogel Oscillator. *Sci. Robot.* **2019**, *4* (33), eaax7112.

(8) Gong, J. P.; Katsuyama, Y.; Kurokawa, T.; Osada, Y. Double-Network Hydrogels with Extremely High Mechanical Strength. *Adv. Mater.* **2003**, *15* (14), 1155–1158.

(9) Gong, J. P. Materials Both Tough and Soft. *Science (80-.).* **2014**, *344* (6180), 161–162.

(10) Sun, J.-Y.; Zhao, X.; Illeperuma, W. R. K.; Chaudhuri, O.; Oh, K. H.; Mooney, D. J.; Vlassak, J. J.; Suo, Z. Highly Stretchable and Tough Hydrogels. *Nature* **2012**, *489* (7414), 133–136.

(11) Sun, T. L.; Kurokawa, T.; Kuroda, S.; Ihsan, A. Bin; Akasaki, T.; Sato, K.; Haque, M. A.; Nakajima, T.; Gong, J. P. Physical Hydrogels Composed of Polyampholytes Demonstrate High Toughness and Viscoelasticity. *Nat. Mater.* **2013**, *12* (10), 932–937.

(12) Zhao, X. Multi-Scale Multi-Mechanism Design of Tough Hydrogels: Building Dissipation into Stretchy Networks. *Soft Matter* **2014**, *10* (5), 672–687.

(13) Webber, R. E.; Creton, C.; Brown, H. R.; Gong, J. P. Large Strain Hysteresis and Mullins Effect of Tough Double-Network Hydrogels. *Macromolecules* **2007**, *40*

(8), 2919–2927.

(14) Gong, J. P. Why Are Double Network Hydrogels so Tough? *Soft Matter* **2010**, *6* (12), 2583–2590.

(15) Yan, Y.; Li, M.; Yang, D.; Wang, Q.; Liang, F.; Qu, X.; Qiu, D.; Yang, Z. Construction of Injectable Double-Network Hydrogels for Cell Delivery. *Biomacromolecules* **2017**, *18* (7), 2128–2138.

(16) Luo, F.; Sun, T. L.; Nakajima, T.; Kurokawa, T.; Zhao, Y.; Sato, K.; Ihsan, A. Bin; Li, X.; Guo, H.; Gong, J. P. Oppositely Charged Polyelectrolytes Form Tough, Self-Healing, and Rebuildable Hydrogels. *Adv. Mater.* **2015**, *27* (17), 2722–2727.

(17) Zhang, H. J.; Sun, T. L.; Zhang, A. K.; Ikura, Y.; Nakajima, T.; Nonoyama, T.; Kurokawa, T.; Ito, O.; Ishitobi, H.; Gong, J. P. Tough Physical Double-Network Hydrogels Based on Amphiphilic Triblock Copolymers. *Adv. Mater.* **2016**, *28* (24), 4884–4890.

(18) Tamate, R.; Hashimoto, K.; Horii, T.; Hirasawa, M.; Li, X.; Shibayama, M.; Watanabe, M. Self-Healing Micellar Ion Gels Based on Multiple Hydrogen Bonding. *Adv. Mater.* **2018**, *30* (36), 1802792.

(19) Su, E.; Yurtsever, M.; Okay, O. A Self-Healing and Highly Stretchable Polyelectrolyte Hydrogel via Cooperative Hydrogen Bonding as a Superabsorbent Polymer. *Macromolecules* **2019**, *52* (9), 3257–3267.

(20) Chen, Q.; Zhu, L.; Chen, H.; Yan, H.; Huang, L.; Yang, J.; Zheng, J. A Novel Design Strategy for Fully Physically Linked Double Network Hydrogels with

Tough, Fatigue Resistant, and Self-Healing Properties. *Adv. Funct. Mater.* **2015**, *25* (10), 1598–1607.

(21) Zhang, X. N.; Wang, Y. J.; Sun, S.; Hou, L.; Wu, P.; Wu, Z. L.; Zheng, Q. A Tough and Stiff Hydrogel with Tunable Water Content and Mechanical Properties Based on the Synergistic Effect of Hydrogen Bonding and Hydrophobic Interaction. *Macromolecules* **2018**, *51* (20), 8136–8146.

(22) Long, R.; Mayumi, K.; Creton, C.; Narita, T.; Hui, C. Y. Time Dependent Behavior of a Dual Cross-Link Self-Healing Gel: Theory and Experiments. *Macromolecules* **2014**, *47* (20), 7243–7250.

(23) Guo, J.; Long, R.; Mayumi, K.; Hui, C. Y. Mechanics of a Dual Cross-Link Gel with Dynamic Bonds: Steady State Kinetics and Large Deformation Effects. *Macromolecules* **2016**, *49* (9), 3497–3507.

(24) Mayumi, K.; Marcellan, A.; Ducouret, G.; Creton, C.; Narita, T. Stress-Strain Relationship of Highly Stretchable Dual Cross-Link Gels: Separability of Strain and Time Effect. *ACS Macro Lett.* **2013**, *2* (12), 1065–1068.

(25) Cui, K.; Sun, T. L.; Kurokawa, T.; Nakajima, T.; Nonoyama, T.; Chen, L.; Gong, J. P. Stretching-Induced Ion Complexation in Physical Polyampholyte Hydrogels. *Soft Matter* **2016**, *12* (43), 8833–8840.

(26) Sun, T. L.; Luo, F.; Hong, W.; Cui, K.; Huang, Y.; Zhang, H. J.; King, D. R.; Kurokawa, T.; Nakajima, T.; Gong, J. P. Bulk Energy Dissipation Mechanism for the Fracture of Tough and Self-Healing Hydrogels. *Macromolecules* **2017**, *50* (7), 2923–2931.

(27) Sun, T. L.; Luo, F.; Kurokawa, T.; Karobi, S. N.; Nakajima, T.; Gong, J. P. Molecular Structure of Self-Healing Polyampholyte Hydrogels Analyzed from Tensile Behaviors. *Soft Matter* **2015**, *11* (48), 9355–9366.

(28) Ihsan, A. Bin; Sun, T. L.; Kurokawa, T.; Karobi, S. N.; Nakajima, T.; Nonoyama, T.; Roy, C. K.; Luo, F.; Gong, J. P. Self-Healing Behaviors of Tough Polyampholyte Hydrogels. *Macromolecules* **2016**, *49* (11), 4245–4252.

(29) Taylor, D. L.; in het Panhuis, M. Self-Healing Hydrogels. *Adv. Mater.* **2016**, *28* (41), 9060–9093.

(30) Guo, H.; Sanson, N.; Hourdet, D.; Marcellan, A. Thermoresponsive Toughening with Crack Bifurcation in Phase-Separated Hydrogels under Isochoric Conditions. *Adv. Mater.* **2016**, *28* (28), 5857–5864.

(31) Cui, K.; Sun, T. L.; Liang, X.; Nakajima, K.; Ye, Y. N.; Chen, L.; Kurokawa, T.; Gong, J. P. Multiscale Energy Dissipation Mechanism in Tough and Self-Healing Hydrogels. *Phys. Rev. Lett.* **2018**, *121* (18), 185501.

(32) Li, X.; Cui, K.; Sun, T. L.; Meng, L.; Yu, C.; Li, L.; Creton, C.; Kurokawa, T.; Gong, J. P. Mesoscale Bicontinuous Networks in Self-Healing Hydrogels Delay Fatigue Fracture. *Proc. Natl. Acad. Sci.* **2020**, *117* (14), 7606–7612.

(33) Cui, K.; Ye, Y. N.; Sun, T. L.; Chen, L.; Li, X.; Kurokawa, T.; Nakajima, T.; Nonoyama, T.; Gong, J. P. Effect of Structure Heterogeneity on Mechanical Performance of Physical Polyampholytes Hydrogels. *Macromolecules* **2019**, *52* (19), 7369–7378.

(34) Hammersley, A. P. FIT2D : A Multi-Purpose Data Reduction, Analysis and

Visualization Program. *J. Appl. Crystallogr.* **2016**, *49* (2), 646–652.

(35) Rubinstein, M.; Colby, R. H. *Polymer Physics*; Oxford University Press, 2003.

(36) Ihsan, A. Bin; Sun, T. L.; Kuroda, S.; Haque, M. A.; Kurokawa, T.; Nakajima, T.; Gong, J. P. A Phase Diagram of Neutral Polyampholyte – from Solution to Tough Hydrogel. *J. Mater. Chem. B* **2013**, *1* (36), 4555.

(37) Takeoka, Y.; Berker, A. N.; Du, R.; Enoki, T.; Grosberg, A.; Kardar, M.; Oya, T.; Tanaka, K.; Wang, G.; Yu, X.; Tanaka, T. First Order Phase Transition and Evidence for Frustrations in Polyampholytic Gels. *Phys. Rev. Lett.* **1999**, *82* (24), 4863–4865.

(38) Dobrynin, A. V.; Colby, R. H.; Rubinstein, M. Polyampholytes. *J. Polym. Sci. Part B Polym. Phys.* **2004**, *42* (19), 3513–3538.

(39) English, A. E.; Mafé, S.; Manzanares, J. A.; Yu, X.; Grosberg, A. Y.; Tanaka, T. Equilibrium Swelling Properties of Polyampholytic Hydrogels. *J. Chem. Phys.* **1996**, *104* (21), 8713–8720.

(40) Nakajima, T.; Furukawa, H.; Tanaka, Y.; Kurokawa, T.; Osada, Y.; Gong, J. P. True Chemical Structure of Double Network Hydrogels. *Macromolecules* **2009**, *42* (6), 2184–2189.

(41) Boldon, L.; Laliberte, F.; Liu, L. Review of the Fundamental Theories behind Small Angle X-Ray Scattering, Molecular Dynamics Simulations, and Relevant Integrated Application. *Nano Rev.* **2015**, *6*, 25661.

Table of Contents graphic